

# A NEW THEORY FOR A ROTARY-KILN HEAT EXCHANGER\*

M. IMBER† and V. PASCHKIS‡

(Received December 1961)

**Abstract**—From theoretical considerations, two limits for the length required to achieve a prescribed temperature rise in rotary kilns are established. The “well-mixed” condition represents the lower limit (minimum length), while the “non-mixed” condition represents the upper limit (maximum length). The actual kiln length lies between these two limits. Procedures for the calculation of both limits are presented in the paper.

Results from the “well-mixed” theory agree remarkably well with published data for an existing kiln.

## NOMENCLATURE

The following symbols are used in this paper, and a set of typical dimensions are added in parentheses:

- $a$ , longer side of a rectangle (ft);
- $b$ , shorter side of a rectangle (ft);
- $A$ ,  $\rho_w c_p \bar{r}^2 \omega / k_w$  (dimensionless);
- $A_{m, n}$ , see Appendix (dimensionless);
- $B$ ,  $h_{gw} \bar{r} r_i / k_w [r_0 - r_i]$  (dimensionless);
- $B_{m, n}$ , see Appendix (dimensionless);
- $c_p$ , specific heat at constant pressure (Btu/lb °F);
- $C$ ,  $h_{gw} \bar{r} r_i / k_w [r_0 - r_i]$  (dimensionless);
- $E$ ,  $w c_p$  (Btu/h °F);
- $h$ , boundary conductance (heat-transfer coefficient) (Btu/ft<sup>2</sup> h °F);
- $\bar{h}$ , modified boundary conductance, see equation (20) (Btu/ft<sup>2</sup> h °F);
- $J$ , see Appendix (dimensionless);
- $K$ , see Appendix (dimensionless);
- $k$ , thermal conductivity (Btu/ft h °F);
- $L$ , kiln length (ft);
- $m, n$ , summation indices;
- $Q$ , rate of heat transferred (Btu/h ft);

- $Q_1$ , rate of heat loss from exposed kiln wall (Btu/h ft);
- $Q_2$ , rate of heat loss from covered kiln wall (Btu/h ft);
- $R$ , see Appendix (dimensionless);
- $r$ , kiln-wall radius (ft);
- $\bar{r}$ , mean kiln-wall radius  $\bar{r} = (r_0 + r_i)/2$  (ft);
- $S$ , see Appendix (dimensionless);
- $T(\theta)$ , temperature measured at angle  $\theta$  (°F);
- $T(L)$ , temperature measured at  $L$  (°F);
- $T(0)$ , temperature measured at  $z = 0$  (°F);
- $v$ , axial velocity of the charge (ft/h);
- $w$ , weight flow (lb/h);
- $x, y$ , Cartesian co-ordinates (ft);
- $z$ , distance measured along kiln bed (ft).

## Greek symbols

- $\alpha$ ,  $A/2$  (dimensionless);
- $\beta$ ,  $[(A/2)^2 + B]^{1/2}$  (dimensionless);
- $\gamma$ ,  $[(A/2)^2 + C]^{1/2}$  (dimensionless);
- $\theta$ , angle (rad);
- $\theta_0$ , included angle of the charge (deg or rad);
- $\mu$ ,  $(1/E_c) - (1/E_g)$  (h °F/Btu);
- $\rho$ , density (lb/ft<sup>3</sup>);
- $\lambda$ , see equation (8) (Btu/h ft °F);
- $\omega$ , angular velocity of the rotating kiln wall (rev/h);
- $\psi$ ,  $(m\pi/a)^2 + (n\pi/b)^2$  (ft<sup>-1</sup>);
- $\varphi$ ,  $E_g/E_c$  (dimensionless).

## Subscripts

- $c$ , charge;
- $i$ , inside;

\* Based on a dissertation undertaken in partial fulfillment of the requirements for the degree of Doctor of Engineering Science in Mechanical Engineering at Columbia University, New York 27.

† Associate Professor, Department of Mechanical Engineering, Polytechnic Institute of Brooklyn, 333 Jay Street, Brooklyn, New York.

‡ Professor in Mechanical Engineering and Director of the Heat and Mass Flow Laboratory, Columbia University, New York 27.

<i>g</i> ,	gas;
<i>o</i> ,	outside;
<i>w</i> ,	wall;
1,	exposed section of kiln wall;
2,	covered section of kiln wall;
<i>gw</i> ,	gas to wall;
<i>gc</i> ,	gas to charge;
<i>wa</i> ,	wall to ambient;
<i>wc</i> ,	wall to charge;
<i>re</i> ,	re-radiated.

### I. INTRODUCTION

WHILE the performance of a rotary kiln depends critically on the heat transfer, analytical studies of the thermal behavior of kilns are practically non-existent. Instead, analysis of the over-all performance of existing units led in the past to several conflicting design criteria, none of which included the heat-transfer aspects of the kiln. In a previous paper [1] the authors presented a theoretical treatment of the heat-transfer considerations. Briefly, it was stated that the exact analytical expressions for the gas and charge temperatures in a rotary kiln are too complex for practical use, and that it therefore seems more desirable to establish equations for two limits for these temperatures. These limits are defined as the "well-mixed" and the "non-mixed" conditions; the terms are derived from the importance attributed to the mixing of the charge through tumbling. In the "well-mixed" kiln, the tumbling is assumed to be so perfect that the charge has a uniform temperature at any cross-section. For this case, the above-mentioned paper presents expressions for the gas, kiln wall, and charge temperatures. In the "non-mixed" condition, tumbling is assumed not to occur at all; instead, a slug of charge material, having the cross-section of the filled part of the drum, travels along the length of the kiln: under these conditions, the temperature of the charge is not uniform at any cross-section. The present paper starts with a brief review of the previously developed equations, which are then improved by inclusion of expressions for wall losses and re-radiation. After expressions for the "non-mixed" condition performance are derived, data from an existing kiln are compared with results obtained by both methods of calculation ("well-mixed" and "non-mixed").

### II. REVIEW OF THE "WELL-MIXED" CONDITION

In deriving the equations for the "well-mixed" conditions [1], the authors considered the rotary kiln as a heat exchanger with the following modifications. There is no wall separating the two fluid streams, gas and charge, which are in heat exchange, and the wall which encompasses both streams is rotating. This outer rotating wall serves as an additional heat-flow path, since it transports the heat which it receives from the hot gases to the underside of the charge: this heat transport occurs in part by conduction, and in part by storing heat in each particle of wall while it is exposed to the gas and giving it off while it is in contact with the charge. In Fig. 1, the heat-flow paths for a typical section in the rotary kiln are traced.

From energy balances for a differential element  $dz$ , of kiln length, the differential equations for the wall, gas and charge temperatures may be obtained: the solutions to these equations are complicated functions of dimensionless parameters  $\alpha$ ,  $\beta$ ,  $\gamma$  and  $\theta_0$ , the meaning of which are explained in the nomenclature. By definition  $\beta = (\alpha^2 + B)^{1/2}$  and  $\gamma = (\alpha^2 + C)^{1/2}$ ; writing the square roots in series form is permissible if  $(B/\alpha^2)^2 \leq 1$  and  $(C/\alpha^2)^2 \leq 1$ :

$$\beta = \alpha + \frac{B}{2\alpha} - \frac{1}{8} \frac{B^2}{\alpha^3} + \dots \quad (1)$$

and

$$\gamma = \alpha + \frac{C}{2\alpha} - \frac{1}{8} \frac{C^2}{\alpha^3} + \dots \quad (2)$$

By examination of the physical properties of actual kilns, one finds that  $B \ll 2\alpha^2$  and  $C \ll 2\alpha^2$ ; consequently, the series expansion is allowable and, all terms beyond the second in equations (1) and (2) may be neglected. Thus, simplified equations (3) and (4) are obtained:

$$\beta = \alpha + \frac{B}{2\alpha} \quad (3)$$

$$\gamma = \alpha + \frac{C}{2\alpha} \quad (4)$$

Disregarding the re-radiation from the exposed part of the wall through the translucent combustion gases and the heat losses from the outside surface of the kiln wall, the authors obtained the following equations for the

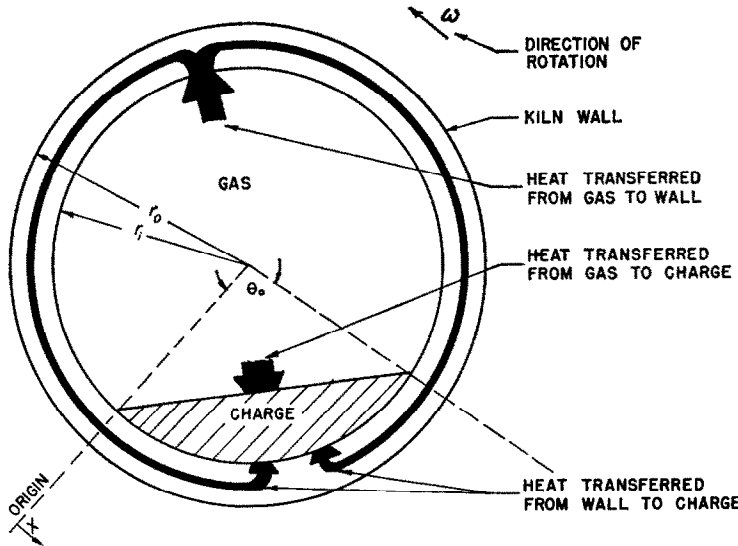


FIG. 1. Schematic diagram showing the heat-flow paths and nomenclature for a typical section in a rotary kiln.

temperatures [1], using the approximate expressions equations (1) and (2) for  $\beta$  and  $\gamma$ : for the portion of the wall covered by the charge,

$$\frac{T_2(\theta, z) - T_g(z)}{T_c(z) - T_g(z)} = \frac{-B(2\pi - \theta_0)}{B(2\pi - \theta_0) + C\theta_0} e^{-(C/2\alpha)\theta_0} + 1, \quad 0 \leq \theta \leq \theta_0, \quad (5a)$$

for the exposed portion of the kiln wall washed by the hot gases,

$$\frac{T_1(\theta, z) - T_g(z)}{T_c(z) - T_g(z)} = \frac{C\theta_0}{B(2\pi - \theta_0) + C\theta_0} e^{-(B/2\alpha)\theta_0}, \quad \theta_0 \leq \theta \leq 2\pi, \quad (5b)$$

for the gas,

$$T_g(z) = T_g(L) \left\{ \frac{-\varphi + e^{\mu\lambda z}}{-\varphi + e^{\mu\lambda L}} \right\} + T_c(0) \left\{ \frac{1 - e^{\mu\lambda z}}{1 - \varphi} - \frac{[1 - e^{\mu\lambda L}][-\varphi + e^{\mu\lambda z}]}{[1 - \varphi][-\varphi + e^{\mu\lambda L}]} \right\}, \quad (6)$$

and for the charge,

$$T_c(z) = T_g(L) \left\{ \frac{-\varphi[1 - e^{\mu\lambda z}]}{-\varphi + e^{\mu\lambda L}} \right\} + T_c(0) \left\{ \frac{1 - e^{\mu\lambda z}}{1 - \varphi} - \frac{[1 - e^{\mu\lambda L}][-\varphi + e^{\mu\lambda z}]}{[1 - \varphi][-\varphi + e^{\mu\lambda L}]} + \frac{[1 - e^{\mu\lambda L}]e^{\mu\lambda z}}{-\varphi + e^{\mu\lambda L}} + e^{\mu\lambda z} \right\}, \quad (7)$$

where

$$\varphi = \frac{E_g}{E_c}$$

and

$$\lambda = h_{gc}2r_i \sin \frac{\theta_0}{2} + \left[ \frac{1}{h_{wc}r_i\theta_0} + \frac{1}{h_{gw}r_i(2\pi - \theta_0)} \right]^{-1} \quad (8)$$

The expression for  $\lambda$ , equation (8), is independent of the physical properties of the kiln as well as of its rotational speed. A formulation for  $\lambda$  may be obtained which includes the rotational speed, the kiln-wall thermal conductivity, and thickness; however, in the previous investigations by the authors [1], the contribution of these quantities is shown to be of second-order effect only.

### III. INCLUSION OF HEAT LOSSES AND RE-RADIATION

If  $Q_1$  and  $Q_2$  represent the average rates of steady-state heat losses per foot of kiln length of the uncovered and covered portions of the kiln wall, respectively, and  $Q_{re, wc}$  the rate of internal heat re-radiated from the exposed wall to the charge's surface, it is possible to extend the "well-mixed" theory to include these effects in the following manner. For a differential element of kiln length  $dz$ , the heat-flow paths

for the uncovered and covered portions of the kiln wall are shown in Figs. 2 and 3: the terms 1 and 2 represent the heat conducted in the wall; terms 3 and 4, the heat transported by the rotating wall. From the energy balance for the hot gases, the differential quantity of heat lost by the gas per unit time,  $dQ_g$ , is

$$dQ_g = dQ_c + Q_1 + Q_2 \quad (9)$$

where

$$E_g \frac{d}{dz} T_g(z) = dQ_g \quad (10)$$

and

$$E_c \frac{d}{dz} T_c(z) = dQ_c. \quad (11)$$

Subtracting equation (11) from equation (10), and substituting equation (9) into the result, one obtains the following relationship:

$$\frac{d}{dz} \{T_g(z) - T_c(z)\} = \mu dQ_g + \frac{Q_1 + Q_2}{E_c}. \quad (12)$$

Equation (12) may be further simplified, since

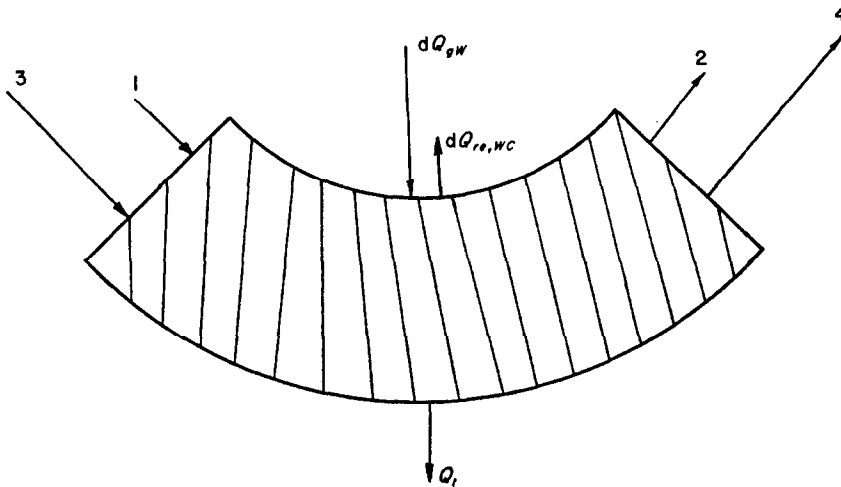


FIG. 2. Heat-flow paths for the exposed portion of the kiln wall.

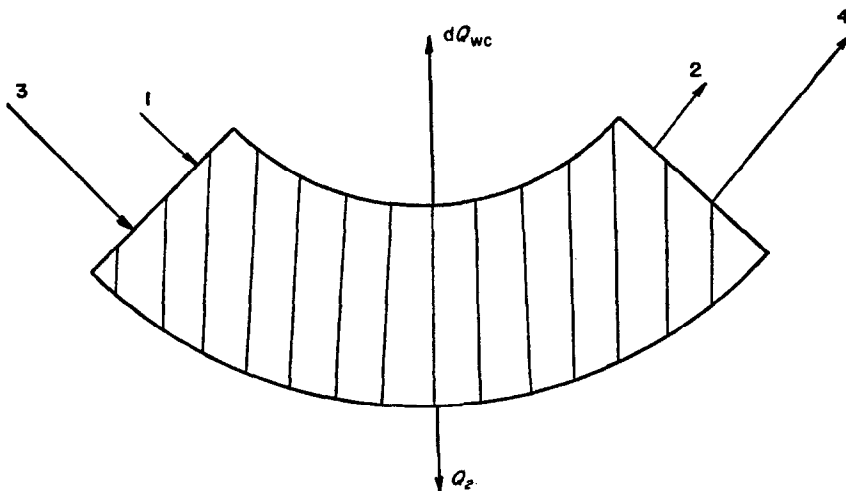


FIG. 3. Heat-flow paths for the covered portion of the kiln wall.

the rate of heat lost by the gas in  $dz$  is also equal to

$$dQ_g = dQ_{gc} + dQ_{gw} \quad (13)$$

As shown in Fig. 2, the rate of heat flow to the exposed wall from the gases in  $dz$ ,  $dQ_{gw}$  is

$$dQ_{gw} = dQ_{re, wc} + Q_1 + [-1 - 3 + 2 + 4] \quad (14)$$

Substituting equations (13) and (14) into equation (12) establishes equation (15):

$$\frac{d}{dz} \{T_g(z) - T_c(z)\} = \mu \{dQ_{gc} + dQ_{re, wc} + [-1 - 3 + 2 + 4]\} + \frac{Q_1}{E_g} + \frac{Q_2}{E_c} \quad (15)$$

From the equations for the temperatures in the wall, and the defining equations (20–22), the bracketed term may be replaced by

$$\{dQ_{gc} + dQ_{re, wc} + [-1 - 3 + 2 + 4]\} = \left\{ 2\bar{h}_{gc}r_i \sin \frac{\theta_0}{2} + \left[ \frac{1}{\bar{h}_{wc}r_i\theta_0} + \frac{1}{\bar{h}_{gw}(2\pi - \theta_0)r_i} \right]^{-1} \right\} \{T_g(z) - T_c(z)\} \quad (16)$$

This substitution, equation (16), is discussed in the earlier paper by the authors [1]. Performing the required integration, one obtains the dimensionless temperature difference:

$$\frac{T_g(L) - T_c(L)}{T_g(0) - T_c(0)} = \exp \left\{ L \left[ \mu \lambda + \frac{Q_1}{E_g(T_g - T_c)_{avg.}} + \frac{Q_2}{E_c(T_g - T_c)_{avg.}} \right] \right\} \quad (17)$$

Since the thickness of the wall is small in comparison to its perimeter, the circumferential heat flow may be disregarded. Consequently, for the exposed portion of the kiln wall, i.e. area of the wall exposed to the hot gases, the rate of heat losses  $Q_1$  may be approximated by the expression

$$Q_1 = \left\{ 2\pi [T_g - 60]_{avg.} \left/ \frac{1}{\bar{h}_{gw}r_i} + \frac{1}{\bar{h}_{wa}r_o} \right. + \frac{\ln(r_o/r_i)}{k_w} \right\} \left\{ \frac{2\pi - \theta_0}{2\pi} \right\} \quad (18)$$

where  $T_g$  is the arithmetic mean of the gas entrance and exit temperatures, and the ambient

temperature is 60°F. Similarly, the rate of heat losses from the covered portion of the kiln wall to the ambient  $Q_2$  may be approximated by

$$Q_2 = \left\{ 2\pi [T_c - 60]_{avg.} \left/ \frac{1}{\bar{h}_{wc}r_i} + \frac{1}{\bar{h}_{wa}r_o} \right. + \frac{\ln(r_o/r_i)}{k_w} \right\} \left\{ \frac{\theta_0}{2\pi} \right\} \quad (19)$$

where  $T_c$  is the arithmetic mean of the charge entrance and exit temperatures. In the difference  $[T_g - T_c]_{avg.}$  appearing in the exponential term of equation (17), the arithmetic means of entrance and exit values have to be taken for gas as well as charge temperature. The quantity  $\lambda$  has the same general form as in equation (8); however, the boundary conductances  $h_{gc}$ ,  $h_{gw}$  and  $h_{wc}$  are replaced by modified values  $\bar{h}_{gc}$ ,  $\bar{h}_{gw}$  and  $\bar{h}_{wc}$  and the dimensionless numbers  $\beta$  and  $\gamma$  are changed accordingly.

The modified boundary-conductance values are defined by equations (20–22). For the exposed portion of the kiln wall, as shown in Fig. 2,

$$Q_{gw} - Q_1 - Q_{re, wc} = \bar{h}_{gw}r_i [2\pi - \theta_0] [T_g(z) - T_i(z)] \quad (20)$$

where the left-hand side of the equation represents the rate of heat received by the kiln wall. The quantity  $Q_{re, wc}$  is the heat that is radiated by the surface of the exposed kiln wall to the charge's surface. The modified boundary-conductance value  $\bar{h}_{gw}$  equals the boundary conductance  $h_{gw}$ , when  $Q_1$  and  $Q_{re, wc}$  are zero; the modified boundary conductance can of course never be negative, but is usually less than the boundary conductance  $h_{gw}$ . From its definition,  $\bar{h}_{gw}$  can be interpreted as a measure of the net energy received by the wall. The total heat received by the charge through its surface exposed to the hot gases is

$$Q_{gc} + Q_{re, wc} = \bar{h}_{gc}2r_i \sin \frac{\theta_0}{2} [T_g(z) - T_c(z)] \quad (21)$$

where  $\bar{h}_{gc}$  is greater than the conventional heat-transfer coefficient  $h_{gc}$ . For the covered portion of the kiln wall

$$Q_{wc} + Q_2 = \bar{h}_{wc}r_i\theta_0 [T_c(z) - T_c(z)] \quad (22)$$

which is consistent with the previous definitions:  $\bar{h}_{wc}$  is never negative, and it is a measure

of the total energy transferred by the covered portion of the wall. A further discussion of these relationships appears in Section VII.

#### IV. THE "NON-MIXED" CONDITION

As stated above, for the "non-mixed" condition the charge is considered to move down the kiln axis as a slug having the cross-section occupied by the charge in the kiln, and possessing a finite thermal conductivity. In order to solve the "non-mixed" problem, three simplifying assumptions are made. Firstly, instead of starting the computation from the gas temperature, the surface temperatures are assumed to be known. Without the information regarding these temperatures, it is assumed that the exposed surface has the gas temperature, and the covered surface the wall temperature, as determined for the "well-mixed" condition: i.e. the temperatures from equations (6) and (5a) respectively are used. Secondly, the thermal conductivity of the charge in the  $z$ -direction is disregarded, and thirdly the cross-section of the charge is assumed to be a rectangle as shown in Fig. 4, rather than a segment.

Consider a differential element of charge material of lengths,  $dx$ ,  $dy$ ,  $dz$ , through whose faces heat is flowing, and in the axial direction,  $z$ -direction, there is an additional mass transport.

From the energy balance for this differential element, the following differential equation describing the steady-state temperature in the charge is obtained:

$$\frac{\partial^2 T_c}{\partial x^2} + \frac{\partial^2 T_c}{\partial y^2} = \frac{\rho_c c_{p_c} v}{k_c} \frac{\partial T_c}{\partial z}. \quad (23)$$

A heat exchanger, and correspondingly a kiln, can be considered as a transient phenomenon for an observer located in and traveling with the fluid or charge; or one may consider the problem as a steady state for an observer on the kiln wall. For him the charge temperature at any cross-section in the kiln does not vary with time; consequently time does not appear as an additional variable in equation (23).

For a rectangle having sides  $a$  and  $b$ , and an initial temperature of  $T_c(0)$ , the boundary conditions are

$$\left. \begin{aligned} T_c(x, y, 0) &= T_c(0) \\ T_c(0, y, z) &= \text{mean of } T_2(\theta, z) \\ &\quad \text{over the angle } \theta_0 \\ T_c(a, y, z) &= \text{mean of } T_2(\theta, z) \\ &\quad \text{over the angle } \theta_0 \\ T_c(x, 0, z) &= \text{mean of } T_2(\theta, z) \\ &\quad \text{over the angle } \theta_0 \\ T_c(x, b, z) &= T_g(z) \end{aligned} \right\} \quad (24)$$

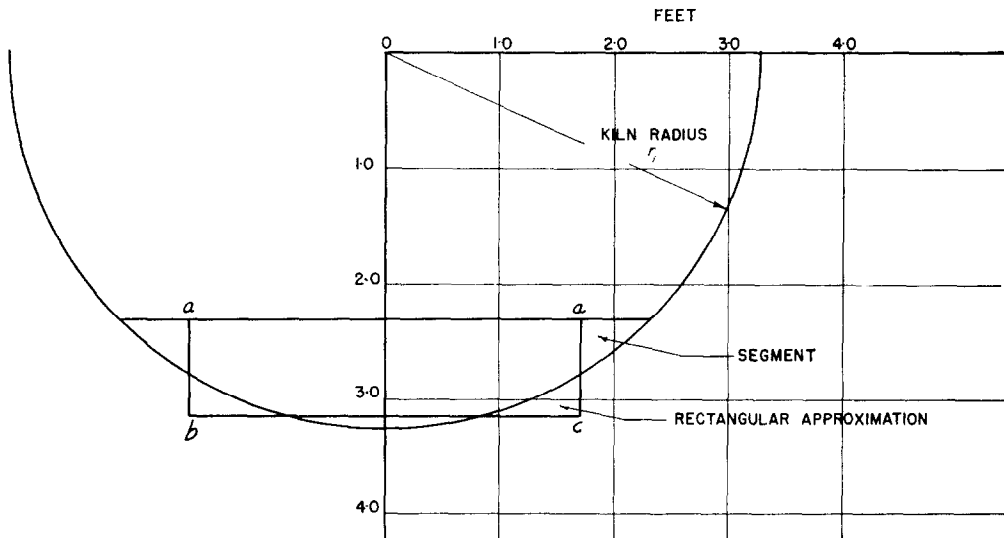


FIG. 4. Rectangular approximation for charge shape in stages 6 and 7.

where the origin of the Cartesian co-ordinate system  $(x, y)$  is chosen so that it coincides with the lower left-hand corner of the rectangle. In essence, the mathematical problem to be solved is that of a rectangle with different temperatures on the several faces, the temperatures varying with  $z$  and therefore with time. The solution is obtained by using Duhamel's theorem. The solution of equation (23) with boundary conditions of equation (24) is found by applying the principle of superposition:

programming the equations for a digital computer.

V. LIMITATIONS OF CALCULATIONS

The procedures both for the "well-mixed" and the "non-mixed" conditions are based on a knowledge of the "modified" boundary conductance as defined by equations (20-22). In order to determine these modified conductances, the heat reradiated from the furnace wall to the charge ( $Q_{re, wc}$ ) and the heat losses ( $Q_1$  and  $Q_2$ )

$$\begin{aligned} \frac{T_c(x, y, z)}{T_c(0)} = & \frac{16}{\pi^2} \sum_{m=1,3,5}^{\infty} \sum_{n=1,3,5}^{\infty} \frac{1}{nm} \sin \frac{m\pi x}{a} \sin \frac{n\pi y}{b} \exp(-k_c z\psi/\rho_c c_{pe} v) \\ & + R + S \exp(\mu\lambda z) + \frac{4}{\pi} [J - R + (K - S) \exp(\mu\lambda z)] \sum_{m=1,3,5}^{\infty} \frac{\sin(m\pi x/a) \sinh(m\pi y/a)}{m \sinh(m\pi b/a)} \\ & + \sum_{n=1,2,3}^{\infty} \sum_{m=1,3,5}^{\infty} A_{mn} \sin \frac{m\pi x}{a} \sin \frac{n\pi y}{b} \left\{ (J + K) \exp(-k_c z\psi/\rho_c c_{pe} v) + \frac{K\mu\lambda}{\mu\lambda + k_c\psi/\rho_c c_{pe} v} \right. \\ & \left. [\exp(\mu\lambda z) - \exp(-k_c z\psi/\rho_c c_{pe} v)] \right\} \\ & + \sum_{n=1,2,3}^{\infty} \sum_{m=1,3,5}^{\infty} B_{mn} \sin \frac{m\pi x}{a} \sin \frac{n\pi y}{b} \left\{ (R + S) \exp(-k_c z\psi/\rho_c c_{pe} v) + \frac{S\mu\lambda}{\mu\lambda + (k_c\psi/\rho_c c_{pe} v)} \right. \\ & \left. [\exp(\mu\lambda z) - \exp(-k_c z\psi/\rho_c c_{pe} v)] \right\}. \end{aligned} \tag{25}$$

The expressions for  $J, K, R, S, A_{mn}$  and  $B_{mn}$  are shown in the Appendix. The large number of complicated terms appearing in equation (25) makes numerical evaluation of the charge temperature time consuming, particularly because the arguments in the exponent decrease, and with decreasing argument the required number of terms increases. Usually it is required to compute the length  $z$  for a desired charge exit temperature; since the variable  $z$  appears as an implicit function, a closed solution cannot be expected. Instead, values of  $z$  are assumed, the temperatures calculated and a curve of  $T$  vs.  $z$  is plotted; from this curve the value of  $z$  desired to achieve a given value of temperature,  $T$ , is read. The numerical work can be reduced by

must be known. While the heat losses can be readily determined, if the outside shell temperature is known, there is, to date, insufficient information available for a determination of  $Q_{re, wc}$ .

The procedures presented in this paper are therefore usually applicable only as approximations, disregarding the re-radiation. Although the outside shell temperature of the kiln is not unknown *a priori*, the rate of heat losses can be included in the computation by a method of successive approximations. The calculation procedures for the several conditions ("well-mixed", "non-mixed", re-radiation and heat losses, etc.) are explained in the several parts of Section VI.

## VI. COMPARISON WITH ACTUAL KILN DATA

### 1. Review of Previous Work

In the light of the several necessary assumptions in the present computing procedure, it seemed desirable to compare the performance predicted by the new computing procedure with results obtained in practice. Only one set of papers reporting empirical data was found which appears usable for comparison—that of Gilbert [2–4]. Gilbert, however, did not measure all items which would be important for a comparison, but instead measured only a few items and, by a lengthy computing procedure which is not always fully explained, arrives at those items used here for comparison. Thus a brief indication of Gilbert's procedure is presented.

In Gilbert's investigation, the temperatures of the gas and charge are determined for a counter-flow, wet-process, rotary cement kiln. Gilbert considers the kiln to be composed of a series of connected regions described as follows: "drying" with the charge temperature reaching but not exceeding 212°F, "raising temperature" with the charge temperature increasing from 212 to 1300°F, followed by regions where endothermic and exothermic reactions take place. Variations in the charge temperature at any cross-section are not considered: only average temperatures are reported. The present paper will utilize the information provided in the region, the purpose of which is described by Gilbert as "raising temperature".

For computational purposes, Gilbert now proceeds to subdivide each region into stages. In particular, the region for "raising temperature" is divided into four stages, and in each of these four stages the charge temperature increases by an equal amount. The next task is to compute the gas temperatures. These Gilbert determines on the basis of the following heat balance for each stage:

$$(a) \text{ Decrease of heat content of gas} = (\text{Increase of heat content of charge}) + (\text{Heat losses from the shell}).$$

As yet a direct computation of gas temperatures and stage lengths is not possible because of the heat transport in the rotating-kiln wall. Thus the following, additional, relationships for each stage must be considered:

$$(b) \text{ Decrease of heat content of gas} = (\text{Heat flow into exposed surface of charge}) + (\text{Heat flow into exposed part of wall});$$

$$(c) \text{ Heat flow into exposed part of wall} = (\text{Heat loss from shell}) + (\text{Heat flow transmitted to bottom (covered) part of charge}) + (\text{Heat re-radiated from exposed part of wall to exposed charge surface}).$$

These several relationships lead to complicated equations. In order to overcome these difficulties, Gilbert uses a method of successive approximations, as follows. First he postulates a fixed but unknown ratio  $\eta$  of heat losses from the shell to the total heat increase of the charge in each stage. Now, assuming a value for  $\eta$ , and using the end temperatures of the charge (which temperatures are used to define the several stages), Gilbert is able to determine the temperature drop of the gas stream. By proceeding from stage to stage, and remembering that the gas exit temperature for the kiln is known, he finds for each stage both entrance and exit gas temperatures. Essentially this procedure represents one application of the heat balance, item (a), to each stage.

The next step is to find the average temperatures for the covered and uncovered portions of the kiln for each stage. Since the rotating kiln wall transports heat from its exposed section to the covered portion, the wall temperature varies circumferentially. In his analysis, Gilbert avoids this difficulty by introducing the assumption that the differences of the average temperatures of the covered and uncovered sections of the wall can be equated to a simple expression involving only the average temperature difference between the gas and charge, and a constant called the "lining storage factor". The introduction of the "lining storage factor" is to account for the effect of the rotating wall; however, Gilbert does not present a rigorous justification for this assumption.

Since the heat received by the exposed portion of the kiln wall must be equal to the amount it gives off, a trial-and-error method is developed by Gilbert to find the average, exposed-wall temperature. In this heat balance, item (c), for the heat transfer by radiation and convection, radiant-gas emissivity values are used for the



former and an empirical relationship for the heat-transfer coefficient for the latter. Also, surprisingly, Gilbert considers that heat is transferred from the covered portion of the kiln wall to the underside of the charge  $Q_{wc}$ , not by conduction but by thermal radiation. The heat losses from the shell are computed from the expression for radial conduction through the kiln wall. This value for the heat losses must be the same as the value obtained from the definition of  $\eta$ . If it is not, then a new value of  $\eta$  is selected and the computations, as outlined, are repeated.

From the heat balance between the gas stream and the exposed kiln wall, item (b), the kiln length associated with each stage can now be computed. The value of the individual quantities of heat transferred per foot of kiln length ( $Q_{gw}$ ,  $Q_{gc}$ ) are known; consequently the sum of these quantities, when divided into the

total heat lost by the gas stream per stage, determines the required stage length.

It is well to note that the heat-flow quantities are not used to determine the respective temperatures of the gas and charge, but rather the kiln lengths for the various stages.

In conclusion, Gilbert's computational procedure is a long program, the justification of which is based upon his industrial experience. Certainly, the manner by which he arbitrarily increases the charge temperature is questionable, since the heat-transfer coefficients to the charge should be used to determine the temperature increases. Equally dubious is the use of the various constants such as the lining storage factor and shell loss fraction.

The theoretical presentation in the current paper couples the gas-temperature drop to the charge-temperature rise through heat-transfer considerations. No assumptions are made

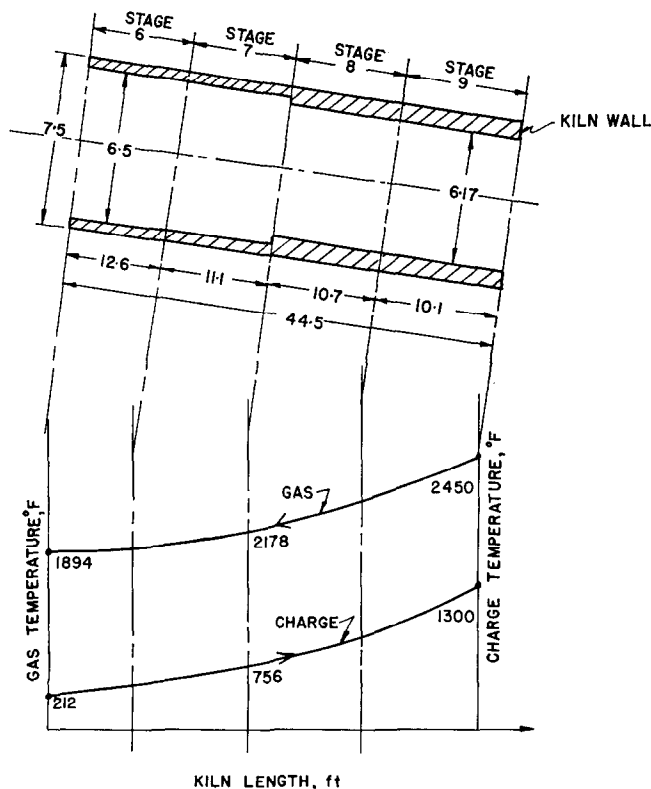


FIG. 5. Schematic sketch of Gilbert's kiln and its temperature.

regarding the charge-temperature increase in the stages under consideration. Furthermore, the expressions for the wall temperatures, exposed and covered, are derived from analysis. In addition, the iterative procedure, as developed in the present paper, converges quite rapidly.

### 2. Data for Gilbert's Rotary Kiln

The method of calculation presented in this paper holds for a dry kiln. In order to use Gilbert's data for comparison, a region in Gilbert's kiln is selected which bears the closest resemblance to a theoretical dry kiln, a region where the chemical reactions are negligible, and the evaporation of the water from the wet slurry has been completed.

Thus stages 6-9 of Gilbert's kiln are chosen, and according to his paper these serve only to raise the temperature of the dry raw material. The gas enters stage 9 (see Fig. 5), at a temperature of 2450°F, and emerges from stage 6 at a temperature of 1894°F. The charge traveling in the opposite direction enters stage 6 at 212°F

and emerges at the end of stage 9 at 1300°F. The kiln is sloped at 1 in 24, and the kiln wall rotates at 1.2 rev/min. With the help of the additional information listed in Tables 1 and 2, the results of the "well-mixed" and "non-mixed" conditions are compared with the aforementioned data

As shown in Fig. 5, stages 6 and 7 have a different diameter from stages 8 and 9. Therefore calculations based on the "well-mixed" theory will be made separately for each pair of stages. Thus the four stages are replaced by two kilns, and in each case for the given section length, the temperatures of the gas and charge are computed at the end of stage 7 (or beginning of stage 8). A second computation is made which determines the kiln lengths necessary to attain a charge temperature of 756°F at the end of stage 7.

In Table 2 the  $\bar{h}$  values are computed by introduction in equations (20-22) of the values for  $Q_{gw}$ ,  $Q_{gc}$ ,  $Q_{wc}$ ,  $Q_1$ ,  $Q_2$ ,  $Q_{re}$ ,  $Q_{reswc}$ ,  $\theta_0$ ,  $r_i$ ,  $T_c$ ,  $T_g$ ,  $T_1$ ,  $T_2$ , from Gilbert's paper. Since  $T_c$ ,  $T_g$ ,  $T_1$  and  $T_2$  are functions of  $z$ , average values are introduced.

Table 1. Data for stages 6-9 computed from Gilbert's information

	Stage 6	Stage 7	Stage 8	Stage 9
$\theta_0$	88.7	88.7	93.2	93.2
$L$	12.6	11.1	10.7	10.1
$E_g$	13 550	13 550	13 700	13 700
$E_c$	5810	5810	5810	5810
$\mu$	-0.985 (10) <sup>-4</sup>	-0.985 (10) <sup>-4</sup>	-0.994 (10) <sup>-4</sup>	-0.994 (10) <sup>-4</sup>

Table 2. Data for stages 6-9 computed from equations (20-22)

	Stage 6	Stage 7	Stage 8	Stage 9
$h_{gw}$	4.14	4.42	4.28	4.06
$h_{gw}$ (avg.)		4.28		4.17
$h_{wc}$	10.95	15.75	21.95	32.1
$h_{wc}$ (avg.)		13.35		27.03
$h_{gc}$	12.03	14.75	18.17	22.5
$h_{gc}$ (avg.)		13.39		20.34
$h_{wa}$		2.0		2.0
$k_w^*$		0.767		0.767
$\lambda$		94.1		132.6
Ambient temp. (°F)		60		60

\* Same as fireclay brick.

### 3. Computations for the "Well-Mixed" Condition

#### A. Based on modified heat-transfer coefficients and kiln losses

The results of the computations described in detail below are shown in Table 3, and the data used for these calculations appear in Tables 1 and 2. The charge and gas temperatures at the end of stage 7 are computed according to the "well-mixed" theory. Stages 6 and 7 together are treated as a rotary kiln 23.7 ft in length whose gases enter at an unknown temperature and leave at a temperature of 1894°F. The charge flowing in the opposite direction, enters at a temperature of 212°F; its exit temperature is to be computed.

Table 3. Comparison of results for stages 6-9

	Stages 6 and 7	Stages 8 and 9
$T_g(0)$	1894°F	
$T_g(L)$		2450°F
$T_c(0)$	212°F	
$T_c(L)$		1300°F
$T_g(L)†$	2192°F	
$T_g(L)‡$	2178°F	
$T_c(L)†$	796°F	
$T_c(L)‡$	756°F	
$T_g(0)†$		2160°F
$T_g(0)‡$		2178°F
$T_c(0)†$		702°F
$T_c(0)‡$		756°F
Heat losses†	623 000 Btu/h	547 500 Btu/h
Heat losses‡	691 000 Btu/h	693 000 Btu/h
$L†$	22.3 ft	19.0 ft
$L‡$	23.7 ft	20.8 ft

† Computed.

‡ Gilbert.

As the initial step in the computation procedure, the average gas and charge temperatures are assumed. These values, when substituted into the expressions for  $Q_1$  and  $Q_2$ , yield the rate of steady-state radial heat losses from the shell; thus all terms appearing on the right-hand side of equation (17) are known. From equation (17) and the heat balance between gas and charge, the charge and gas temperatures at the exit (end of stage 7) may be determined:

$$E_g \{T_g(L) - T_g(0)\} = E_c \{T_c(L) - T_c(0)\} + \{Q_1 + Q_2\}L. \quad (26)$$

Based on these values, new average temperatures

for the gas and charge can be computed. These new temperatures when re-substituted into the expressions for  $Q_1$  and  $Q_2$ , in turn establish a new set of temperatures. This method is repeated until there is little change in the successive values for the computed charge and gas temperatures at the end of stage 7. The charge and gas temperatures as determined by this method are 796 and 2192°F, respectively, as against Gilbert's reported values of 756 and 2178°F (see Table 3). A further comparison may be made between the heat losses reported by Gilbert and those established by calculation. For stages 6 and 7 Gilbert lists the rate of heat losses as 691 000 Btu/h, while the computed heat losses,  $(Q_1 + Q_2)L$ , are 623 000 Btu/h.

To provide an additional test of the "well-mixed" theory the temperatures of the charge at inlet and exit as well as one gas temperature are considered prescribed; e.g. for stages 6 and 7 the prescribed gas exit temperature is the temperature at the beginning of stage 6, and for stages 8 and 9 the prescribed gas inlet temperature is the temperature prevailing at the end of stage 9. The required length is computed and compared with that of the actual kiln. In other words, for stages 6 and 7, how long a kiln is required to raise the charge temperature from 212 to 756°F if the exit gas temperature is 1894°F? The computational procedure is identical to the method described previously, and the results are listed in Table 3. For stages 6 and 7, the computed length is 22.3 ft as against Gilbert's value of 23.7 ft. Although the calculations for the kiln length are rather sensitive to small variations in the gas temperatures, the computation results are in close agreement with the reported data.

A second comparison refers to the combined stages 8 and 9 representing a kiln 20.8 ft long with hot-gas-entrance and charge-exit temperatures of 2450 and 1300°F, respectively. The gas-exit and charge-entrance temperatures are computed by the same method as before; the location of gas exit and charge entrance is the position between stages 7 and 8, as shown in Fig. 5.

#### B. Based on conventional heat-transfer coefficients and no kiln losses

For the previous calculations, the concept of

the modified heat-transfer coefficients is used. Thus, such calculations can be carried out only if the rates of heat flow are established otherwise. Additional computations were also performed with the conventional heat-transfer coefficients  $h_{gc}$ ,  $h_{gw}$ , heat losses being disregarded. The method of calculation is the same as the one used in part A of this computation. Re-radiation from the exposed portion of the kiln wall to the surface of the charge was not considered in these calculations. The results of this computation are compared with Gilbert's values (in brackets) in Table 4, which also includes a comparison of the values for the modified and conventional heat-transfer coefficients. Except for the charge temperature in stages 8 and 9, the temperatures check very well, indicating that at least for Gilbert's kiln it is not necessary to use the modified  $h$  values; the conventional ones yield results in good agreement with Gilbert's data. However, the length, which should be smaller for this kiln than Gilbert's (because in the present calculation losses from the shell are disregarded), turns out to be larger in stages 6 and 7.

Table 4. Results for Gilbert's kiln based upon conventional heat-transfer coefficients,  $h_{gw}$ ,  $h_{gc}$  and no heat losses

	Stages 6 and 7	Stages 8 and 9
$h_{gw}$	4.28	4.17
$h_{gc}$	13.02	15.50
$h_{gc}$	13.39	20.34
$h_{gc}$	9.08	14.1
$h_{wc}$	13.35	27.03
$h_{wc}$	11.29	21.18
$\lambda^\dagger$	85.55	134.8
$T_g(L)^\dagger$	2123°F (2178)	
$T_c(L)^\dagger$	748°F (756)	
$T_g(0)^\dagger$		2177°F (2178)
$T_c(0)^\dagger$		658°F (756)
$L^\dagger$	24.3 ft (23.7)	17.91 ft (20.8)

† Computed.

The conventional coefficients are determined as follows. The gas-side heat-transfer coefficients are obtainable from Gilbert's temperatures and gas volumes. The values, shown in Table 4, are the sum of the convection and radiant heat-transfer coefficients. The former value is com-

puted from the conventional convection formulas involving Prandtl and Reynolds numbers [5]. The latter, the radiation coefficient, is determined if the heat that is radiated from the CO<sub>2</sub> and water vapor is divided by the temperature difference of gas and wall or charge respectively. The respective emissivities and absorptivities are determined from the work published by Hottel [6]. Since no information is available for the heat-transfer coefficient  $h_{wc}$ , it is assumed that this value is the same as the one determined from Gilbert's work.

### C. Method of calculation including wall losses when the modified heat-transfer coefficients are not given

If the conventional heat-transfer coefficients are determinable and the re-radiation term  $Q_{re,wc}$  is neglected, the following iterative procedure yields the gas and charge temperatures.

Firstly, computations are performed for the rotary kiln with no heat losses. From the average wall temperatures, integration of equations (5a, b), with respect to the angle  $\theta$ , the quantities  $Q_{gw}$  and  $Q_{wc}$  may be evaluated in turn.

If the kiln is now considered to have heat losses when the wall temperatures are at the previous values, then, by substitution of the conventional heat-transfer coefficients,  $h_{gw}$  and  $h_{wc}$  into equations (18) and (19), the heat losses may be determined. The modified heat-transfer coefficients follow from equations (21) and (22) when the temperatures are the average temperatures for the stages. It is now a simple matter to compute a new value for  $\lambda$  based upon the modified heat-transfer coefficients: this in turn establishes new values for the gas and charge temperatures. The method is now repeated until convergence is indicated.

In the computations, the conventional heat-transfer coefficients are assumed constants. This is not quite true, since  $h_{gc}$  and  $h_{gw}$  are composed of a radiation component which varies with temperature. The proposed method does not include this effect.

Computations are performed for stages 8 and 9, since Table 4 indicates a larger difference in the charge temperatures. As shown in Table 5, the method appears to converge quickly: final

Table 5. Iteration procedure for computations of gas and charge temperatures for stages 8 and 9

	First step (no heat loss— conventional heat-transfer coefficients condition)	Second step	Third step	Fourth and final step	Gilbert's kiln
$L$	20.8	20.8	20.8	20.8	20.8
$h_{gw}$	15.50	11.25	12.09	11.82	4.17
$h_{gc}$	14.10	14.10	14.10	14.10	20.34
$h_{wc}$	21.18	21.95	21.90	22.20	27.03
$\lambda$	134.8	128.8	130.7	130.6	132.6
$T_o(L)$	2177	2155	2153	2151	2178
$T_o(0)$	658	713	702	701	756
$T_o$ (avg.)	2314	2303	2302	2302	2314
$T_c$ (avg.)	979	1007	1001	1001	1028
$T_1$ (avg.)	1895	1791	1826	1807	1580
$T_2$ (avg.)	1878	1777	1797	1792	1369
$Q_{gw}$	93 000	114 000	106 100	110 000	129 300
$Q_{gc}$	84 300	81 800	82 200	82 200	55 700
$Q_{wc}$	95 400	81 000	84 800	84 200	35 600
$Q_1$	25 750	25 150	25 250	25 200	24 380
$Q_2$	3725	3850	3830	3830	8620

gas and charge temperatures being 2151 and 701°F, respectively.

#### 4. Computations for the "Non-Mixed" Condition

While computations for the "non-mixed" theory are lengthier than those for the "well-mixed" condition, they are still manageable. In the present paper, the calculations according to the "non-mixed" theory are performed for a rotary kiln 23.7 ft long, stages 6 and 7, with a uniform charge entrance temperature of 212°F. The temperature distribution in the charge at the end of stage 7 may be computed from equation (25). Since the severest temperature gradients exist along the center-line of the charge, at  $x = a/2$ , only this temperature variation is computed.

As first step, the segmental shape of the charge is replaced by a rectangle of equal cross-sectional area, as shown in Fig. 4. The dimensions of the rectangle are selected so as to include as much of the original exposed surface of the charge as possible; thus the rectangle's sides are chosen as  $a = 3.41$  ft and  $b = 0.85$  ft.

Since the charge consists of chiefly  $\text{CaCO}_3$ , it is assumed that the thermal conductivity of

the charge equals that of  $\text{CaCO}_3$ ,  $k = 1.3$  Btu/h ft °F. The resulting temperature profile is shown in Fig. 6 where the charge temperature is plotted against the distance  $y$ . The charge temperature decreases from its exposed surface value of 2178°F to a minimum of 530°F at the center,  $y = 0.425$  ft. Beyond this point the temperature steadily increases till it reaches, at the wall, a temperature of 1424°F. It is interesting to note that, for this one example, almost half of the charge, at the center-line, is below the 756°F value reported by Gilbert. This result is in line with the observed phenomenon that the charge at the exit for a poorly designed kiln can deliver a substantial percentage of its particles "raw".

It should be remembered that the curve, Fig. 6, shows the temperature profile in the center of the charge; if similar profiles were drawn near the sides ( $ab$ ,  $ac$  in Fig. 4) the average temperature from the "non-mixed" case would be very close to the temperature from the "well-mixed" case.

#### VII. DISCUSSION AND CONCLUSIONS

Expressions are presented from which either the temperature changes in the gas and charge, or the kiln length necessary for a prescribed

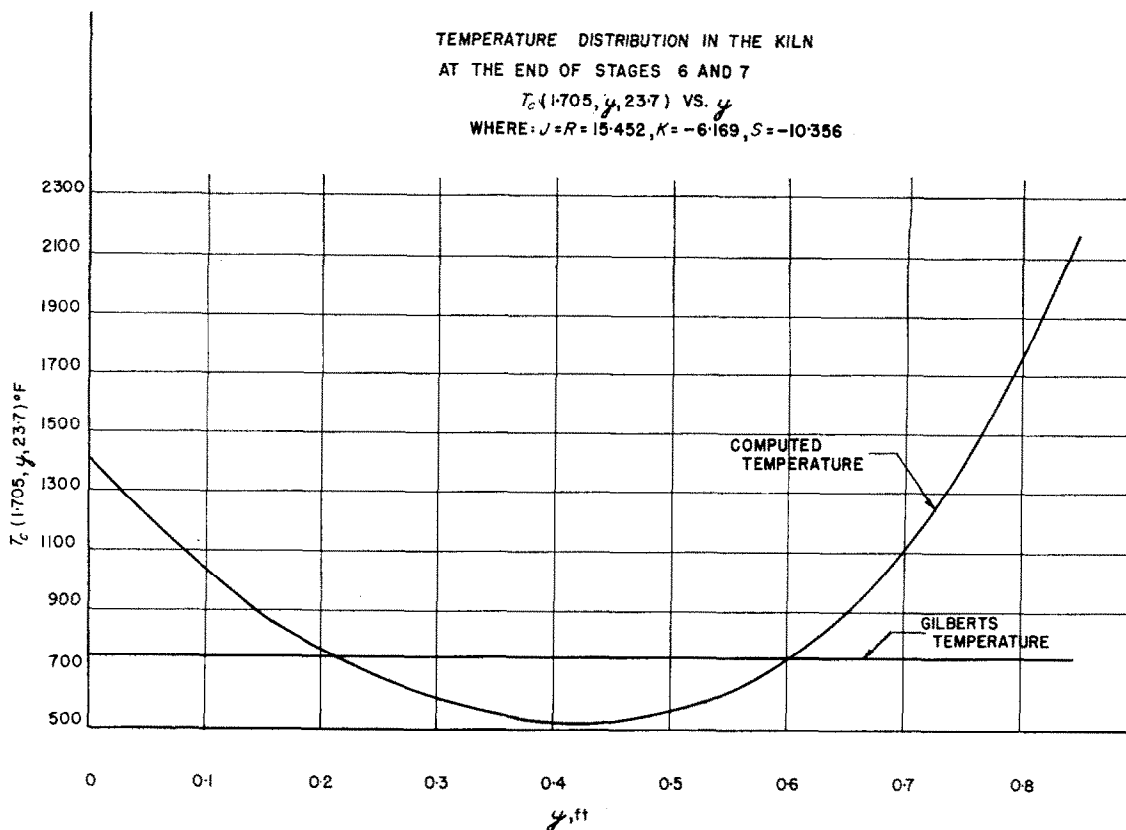


FIG. 6. Temperature distribution in the kiln at the end of stages 6 and 7.

charge temperature can be determined for two limiting conditions: the "well-mixed" and "non-mixed" cases. The length determined from the "well-mixed" theory is a minimal length: ideal mixing is assumed, resulting in temperatures increasing faster than actually occurring; consequently the "well-mixed" condition establishes a lower limit for the required kiln length. In the "non-mixed" condition, there is no tumbling of charge particles; thus the charge temperature rises more slowly than in the actual case, and the required kiln length is longer than in the actual case. The "non-mixed" condition determines an upper limit for the kiln length.

The "modified" heat-transfer coefficients become equal to the "conventional" heat-transfer coefficients when the heat losses and the re-radiated heat becomes zero. Even for this case, the boundary conductance values are not

directly available. As first approximation it appears reasonable to disregard the motion of the charge in determination of the  $h$ -values. One would consider gas velocities for the convection component; moreover it would be necessary to work with average wall and charge surface temperatures. To date, very little information is available in the literature about the heat-transfer coefficient between the covered portion of the kiln wall and the moving charge  $h_{wc}$ . Computations based upon data for two rotary kilns [2-4, 7-9] indicate that  $h_{wc}$  is approximately  $5 h_{gw}$ ; this should be used only as a rule of thumb.

The several modified heat-transfer coefficients were computed from Gilbert's work; consequently the values apply only to the kiln under consideration. In the design of a rotary kiln, the various heat-flow quantities appearing in equa-

tions (20–22) are not known *a priori*. It would be desirable to find a method for computing the modified heat-transfer coefficients from first principles. Until such relationships are developed, it is hoped that kiln manufacturers will accumulate data from existing kilns in order to obtain an empirical correlation for the modified heat-transfer coefficients.

Summarizing some of the findings, one may state that the rotational speed of the kiln has no direct bearing on the heat exchange; also, within practical limits shown in [1], neither thickness of the lining nor its thermal properties have bearing on the thermal performance of the kiln when the heat losses are zero. For the one kiln for which operating data were found in the literature, the theory presented for the "well-mixed" condition yields results remarkably close to the reported values, as may be seen from the three sets of computations listed in Table 3.

For the "non-mixed" condition, the charge-temperature distribution along the center of the charge is obtained. The maximum exit temperature of the charge is 226°F or 30 per cent lower than the reported average of 756°F.

The calculations presented in this and the previous paper are a first step of rationalizing the thermal design of kilns. Further work should include:

- (a) Experimental determination of the  $h_{gc}$  values considering, amongst others, the influence of tumbling, nature of the charge, etc.

- (b) Experimental determination of the  $h_{wc}$  values.  
 (c) Exploration of the re-radiation phenomenon.  
 (d) Expansion of the calculation procedure to include heats of reaction.

#### ACKNOWLEDGEMENTS

The authors wish to take this opportunity to express their gratitude to H. D. Baker, F. Freudenstein and J. H. Weiner, of the Mechanical Engineering Department at Columbia University, for their valuable advice.

#### REFERENCES

1. M. IMBER and V. PASCHKIS, A mathematical analysis of the rotary kiln heat exchanger—1. The well-mixed condition, in *Radex Rundschau* Vol. 4. Oesterreichisch-Amerikanische Magnesit Aktiengesellschaft, Radenthein/Karten (1960).
2. W. GILBERT, Investigations on a slurry drier or calcinator—1. *Cement & Cem. Manuf.* **9**, 115–128 (1936).
3. W. GILBERT, Investigations on a slurry drier or calcinator—2. *Cement & Cem. Manuf.* **9**, 139–154 (1936).
4. W. GILBERT, Investigations on a slurry drier or calcinator—3. *Cement & Cem. Manuf.* **9**, 207–220 (1936).
5. W. H. MCADAMS, *Heat Transmission* (3rd Ed.), p. 219. McGraw-Hill, New York (1954).
6. W. H. MCADAMS, *Heat Transmission* (3rd Ed.), pp. 82–98. McGraw-Hill, New York (1954).
7. H. GYGI, The thermal efficiency of the rotary cement kiln—4. Heat transfer. *Cement & Cem. Manuf.* **11**, 79–84 (1938).
8. H. GYGI, The thermal efficiency of the rotary cement kiln—4 (contd.). Heat transfer. *Cement & Cem. Manuf.* **11**, 133–141 (1938).
9. H. GYGI, The thermal efficiency of the rotary cement kiln—4 (contd.). Heat transfer. *Cement & Cem. Manuf.* **11**, 143–153 (1938).

#### APPENDIX

The expressions for  $J$ ,  $K$ ,  $R$  and  $S$  used in equation (25) are derived from equations (6) and (7) and are:

$$J = \frac{T_g(L)\{-\varphi\}}{T_c(0)\{-\varphi + e^{\mu\lambda L}\}} + \frac{1}{-\varphi + 1} \left\{ 1 + \frac{\varphi[1 - e^{\mu\lambda L}]}{-\varphi + e^{\mu\lambda L}} \right\} \quad (\text{A1})$$

$$K = \frac{T_g(L)}{T_c(0)\{-\varphi + e^{\mu\lambda L}\}} - \frac{1}{-\varphi + 1} - \frac{[1 - e^{\mu\lambda L}]}{[-\varphi + 1][-\varphi + e^{\mu\lambda L}]} \quad (\text{A2})$$

$$J = R \quad (\text{A3})$$

$$S = \left\{ \frac{B(2\pi - \theta_0)(e^{(C\theta_0/2\alpha)} - 1)}{(C\theta_0/2\alpha)[B(2\pi - \theta_0) + C\theta_0]} + 1 \right\} \left\{ \frac{-T_g(L)[- \varphi + 1]}{T_c(0)[- \varphi + e^{\mu\lambda L}] + \frac{1 - e^{\mu\lambda L}}{- \varphi + e^{\mu\lambda L}} + 1} \right\} \\ + \frac{T_g(L)}{T_c(0)} \left\{ \frac{1}{- \varphi + e^{\mu\lambda L}} \right\} - \frac{1}{- \varphi + 1} - \frac{[1 - e^{\mu\lambda L}]}{[- \varphi + 1][- \varphi + e^{\mu\lambda L}]} \quad (\text{A4})$$

For use in equation (25) the constants  $A_{mn}$  and  $B_{mn}$  are the Fourier coefficients

$$A_{mn} = \frac{4}{ab} \int_0^a \int_0^b \left\{ -\frac{4}{\pi} \sum_{m=1,3,5,\dots}^{\infty} \frac{\sin(m\pi x/a) \sinh(m\pi y/a)}{m \sinh(m\pi b/a)} \right\} \sin(m\pi x/a) dx \sin(n\pi y/b) dy \\ = \frac{8(-1)^n}{\pi^2 mn [1 + (bm/an)^2]} \quad (\text{A5})$$

and

$$B_{mn} = \frac{4}{ab} \int_0^a \int_0^b \left\{ -1 + \frac{4}{\pi} \sum \frac{\sin(m\pi x/a) \sinh(m\pi y/a)}{m \sinh(m\pi b/a)} \right\} \sin(m\pi x/a) dx \sin(n\pi y/b) dy \\ = \frac{-8}{nm\pi^2} \{-\cos n\pi + 1\} - \frac{8(-1)^n}{\pi^2 mn [1 + (bm/an)^2]} \quad (\text{A6})$$

**Résumé**—A la suite de considérations théoriques, il est établi que, pour obtenir une élévation de température déterminée dans les fours rotatifs, leur longueur doit être comprise entre deux limites. La condition de “bon mélange” donne la limite inférieure (longueur minimum) tandis que la condition de “non mélange” donne la limite supérieure (longueur maximum). La longueur des fours actuels est comprise entre ces deux limites. Cet article présente une méthode de calcul de ces deux limites.

Les résultats obtenus à partir de la théorie de “bon mélange” concordent remarquablement bien avec les données publiées pour un four réalisé.

**Zusammenfassung**—Um eine vorgeschriebene Temperaturerhöhung in einem Drehofen zu erreichen, ist eine gewisse Weglänge erforderlich. Nach theoretischen Betrachtungen können dafür zwei Grenzwerte angegeben werden. Die Annahme von “Vollmischung” ergibt die untere Grenze (Minimal-Länge); für die Annahme “Nichtmischung” folgt die obere Grenze (Maximal-Länge). Die eigentliche Weglänge im Ofen liegt zwischen diesen beiden Werten. Der Rechengang für beide Grenzen ist angegeben.

Die theoretischen Ergebnisse für “Vollmischung” stimmen erstaunlich gut mit Veröffentlichungen über einen bestehenden Ofen überein.

**Аннотация**—Теоретически установлены два предела длины, требуемой для получения заданного подъема температуры во вращающихся печах. Условие «хорошего перемешивания» соответствует нижнему пределу (минимальной длине), в то время как «отсутствие перемешивания» соответствует верхнему пределу (максимальной длине). Действительно необходимая длина печи лежит между этими двумя пределами. В статье приводится способ нахождения обоих пределов.

Теоретические данные, полученные в предположении «хорошего перемешивания», удивительно хорошо согласуются с опубликованными сведениями о имеющихся печах.